

This work was written as part of one of the author's official duties as an Employee of the United States Government and is therefore a work of the United States Government. In accordance with 17 U.S.C. 105, no copyright protection is available for such works under U.S. Law.

Public Domain Mark 1.0

<https://creativecommons.org/publicdomain/mark/1.0/>

Access to this work was provided by the University of Maryland, Baltimore County (UMBC) ScholarWorks@UMBC digital repository on the Maryland Shared Open Access (MD-SOAR) platform.

**Please provide feedback**

Please support the ScholarWorks@UMBC repository by emailing [scholarworks-group@umbc.edu](mailto:scholarworks-group@umbc.edu) and telling us what having access to this work means to you and why it's important to you. Thank you.

# Effect of high-energy radiation on the electrical and optical characteristics of bioactive glasses

Aria Tauraso,<sup>a</sup> Krishna S. Machuga,<sup>a,b</sup> Joel McAdams,<sup>a</sup> Ching Hua Su,<sup>c</sup>  
Brian Cullum,<sup>a</sup> Tagide deCarvalho<sup>®</sup>,<sup>a</sup> Narasimha S. Prasad<sup>®</sup>,<sup>d</sup> Bradley Arnold,<sup>a</sup>  
Fow-Sen Choa<sup>®</sup>,<sup>a</sup> Kamdeo D. Mandal<sup>®</sup>,<sup>e</sup> and Narsingh Bahadur Singh<sup>®a,\*</sup>

<sup>a</sup>University of Maryland Baltimore County, Baltimore, Maryland, United States

<sup>b</sup>University of Maryland, College Park, Maryland, United States

<sup>c</sup>EM31, NASA Marshall Space Flight Center, Huntsville, Alabama, United States

<sup>d</sup>NASA Langley Research Institute, Hampton, Virginia, United States

<sup>e</sup>Banaras Hindu University, Indian Institute of Technology, Varanasi, Uttar Pradesh, India

**ABSTRACT.** **Significance:** The glassy and crystalline hydroxyapatites that affect the metabolic processes such as tissue growth and healing are affected by the electrical, electro-chemical, and optical properties investigated in this study.

**Aim:** The aim of the present study is to determine effects of high-energy radiation and impurities on the electrical and optical properties of hydroxyapatites responsible for tissue growth and tendency of glass forming ability.

**Approach:** The approach of the study involves synthesis using carbonates, oxides, silicates, phosphates, and borates of parent materials using elevated temperature and low-temperature flux process. High-energy radiation effects were studied by exposing hydroxyapatites with 5  $\mu\text{Ci}$   $\text{Cs}^{137}$   $\gamma$ -ray source. Morphology was studied to determine dissolution and glass formation of additives such as titanium, gallium, and selenium.

**Results:** Irradiation of silicate bio glasses showed huge effects on the electrical characteristics, such as dielectric constant (hence polarity) and resistivity of the materials while optical properties showed insignificant changes. Morphological studies showed transition of faceted to nonfaceted structure.

**Conclusion:** Exposure for the bias voltage of 50 to 1000 mV in the range of 100 to 100000 Hz frequency range showed a large decrease in the dielectric constant and increase in resistivity. The IR and Raman spectra for irradiated glasses exposed for 24 h showed a small change. Morphological results showed that substitution of gallium, magnesium, and/or titanium affects the transition to the glass formation. The addition of selenium showed enormous potential to improve the mixing and glass formation without titanium and gallium precipitates in the matrix.

© 2024 Society of Photo-Optical Instrumentation Engineers (SPIE) [DOI: [10.1117/1.OE.63.3.037105](https://doi.org/10.1117/1.OE.63.3.037105)]

**Keywords:** bioactive glass; bones; borates; hydroxyapatite; borates; phosphates

Paper 20230895G received Sep. 23, 2023; revised Feb. 19, 2024; accepted Feb. 19, 2024; published Mar. 19, 2024.

## 1 Introduction

Hydroxyapatites have been known for a variety of bio and defense applications especially as very good laser hosts. High-temperature Czochralski methods have been developed by Hopkins et al.<sup>1–3</sup> for single crystals for their application as laser host and optical communications.

\*Address all correspondence to Narsingh Bahadur Singh, [singna@umbc.edu](mailto:singna@umbc.edu)

However, the tremendous need for implantation materials to replace the metals in human body and teeth propelled the research to explore hydroxyapatites for bonding to tissues and its growth. Hench et al.<sup>4-9</sup> had proposed that bioactive glasses of this class have great potential and developed several compositions. Their research has demonstrated that among several compositions of bio glasses, 45S5 Bioglass has particularly good properties to bond to bone and soft tissues. In addition, commercial materials listed as “45S5,” “13-93B3,” and “1605” have been developed and discussed for very good bio-activities and applications. The single crystals of hydroxyapatites were characterized for thermal conductivities to estimate heat dissipation. However, even though calcium, phosphate, strontium, and borate ions affect the electrochemical properties, electrical characteristics have significant effects on metabolic properties<sup>10</sup> especially the bonding properties with tissues, the polarity, dielectric, resistivity, and optical effects have attracted more interest to study these properties for hydroxyapatites. Investigations on electrical properties<sup>11-17</sup> indicate that electrical behaviors of calcinated materials create several phenomena, which control the electrical properties. Both Ibrahim et al.<sup>11</sup> and Singh et al.<sup>12</sup> have discussed the detailed mechanisms in bone growth for materials systems and electrical characteristics. They explained the charge transfer in the glass systems using broadband dielectric values. Ibrahim et al.<sup>11</sup> developed the relationship between the hopping time of free ions and dc conductivity. For their materials systems (NiO doped) they demonstrated same-charge transport mechanism and suggested the semiconducting nature for their materials system. Some studies on niobate and other systems have been described;<sup>16</sup> however, electrical properties for compositions close to the bone materials are not discussed in detail. Although the bone regeneration and growth of tissue is overly complex,<sup>18</sup> some studies indicate that electrical properties including surface charges, morphologies, and surface roughness, may influence the biological interactions. This is another reason variation in pH plays important role and the concentration of various ions at the bioactive glass (BG)-fluid interface affects the morphology at the interface. Very similar to the crystal kinetics, local variation in pH varies the growth of tissues at different rates in crystalline bones. However, situations in glassy materials, such as borates and phosphates, are different.

The objectives of this study were to develop compositions similar to that of commercially developed bioactive glasses containing gallium materials and surfaces to prevent wear and corrosion using nano, micro, and bulk materials processed mainly by grain growth method and to measure the effect of high-energy radiation in both high silicate based, and borate based biologically active materials. In some cases, we used selenium to enhance the grain growth and glass transition. The effect of composition and processing was determined to understand the morphology and evaluate thermal characteristics, which may elucidate performance functions that occur because of aging or disease. Detailed focus of the present effort was to develop soft and hard tissues by doping heavy element (gallium) and titanium, which may have less depletion compared to calcium as results of aging and to understand glassy behavior and effect of radiation on properties. The observations on the morphological transition will be shown also in this paper. The detailed investigation by quenching the runs in the middle of heat treatment is still in progress and results will be reported in future.

## 2 Materials and Methods

As described in the previous section the goal was to understand the morphology and effect of some elements on the high-energy radiations on high silicate and high borate glasses especially in samples free from precipitates for good glassy behavior. Several compositions were synthesized for the present study. Table 1 shows the compositions of the mixtures. The focus was to develop various mixtures for study of processing of monolithic silicate glasses containing gallium and titanium (mixture I and II) processed at high temperature and soft hydroxyapatites bones for regrowth and voids fillers in density containing borates and phosphates<sup>19</sup> processed at low temperatures. In the soft glasses (mixture III and IV), we added magnesium and copper as an angiogenesis, which is crucial for tissue generation. Based on our past research results,<sup>19-23</sup> we used selenium to facilitate grain growth at low temperatures. Details of microstructures were studied to evaluate the morphologies, which controls ion release, fills the voids, and helps in regrowth and healing of cracks and voids.

**Table 1** Source materials and compositions of four samples prepared to evaluate effects of titanium copper, magnesium, and selenium and effect of radiations on BGs.

Source materials	Weight of parent components I (g)	Weight of parent components II (g)	Weight of parent components III (g)	Weight of parent components IV (g)
SiO <sub>2</sub>	5.3	5.3	2.12	0.0
CaCO <sub>3</sub>	2.10	2.12	0.824	1.272
Na <sub>2</sub> PO <sub>4</sub>	—	—	0.246	0.378
KOH	1.2	1.2	0.321	0.474
B <sub>2</sub> O <sub>3</sub>	0.221	0.202	2.18	3.274
MgO/MgSO <sub>4</sub>	—	—	0.342	0.534
CuO	—	—	0.012	0.012
Selenium	—	—	0.042	0.066
Sodium carbonate	0.601	0.622	—	—
Ga <sub>2</sub> O <sub>3</sub>	0.410	0.403	—	—
TiO <sub>2</sub>	0	0.611	—	—

Four samples were prepared with the following studies.

1. Samples I and II were prepared to evaluate the effects of the addition of titanium oxide in high silicate glasses with presence of low contents of boron oxide. There was no phosphate content in this class of material.
2. The sample class of II and IV were prepared to evaluate the behavior of glassy phases in glasses containing high borates and phosphates as well as the effect of radiation on these systems. In sample IV, we avoided silicon oxide for making silicate glass. However, we used selenium to process materials at relatively low temperatures. The source materials were similar to that used for synthesizing 1605 bioactive glass. Copper oxide and zinc selenide were added as dopants to the mixtures since some positive effects have been indicated in tissue growth.

The composition I and II were closer to the commercial fibers 1605 and 13-9383 without Cu and Zn impurities.

## 2.1 Synthesis and Pellet Formation

The parent oxides/carbonates were mixed and crushed repeatedly. The listed purity for parent materials was 99.99 + %. We did not purify further before mixing parent components. Repeated grinding and mixing of the powder were done to ensure complete mixing of the components. In some cases, uniform size particles were prepared using a wig-L-bug in a closed quartz ampoule. After thorough mixing, the powders were compressed into a cylindrical pellet using a mechanical pressing device. The pressure for the preparation of pellets was in the range of 7000 to 8000 lb./inch<sup>2</sup>. As shown in Table 1, in samples 3 and 4 we used selenium to facilitate the grain growth at low temperatures. The details of the synthesis by semi-wet and dry methods and heat treatment were similar to that used in preparation of dielectric studies of perovskite materials.<sup>20-23</sup> In samples, I and II, we used titanium oxide and gallium oxide since these have potential to enhance thermal stability. The as-prepared size of pellets was 12 mm in diameter and thickness was 1-2 mm. Figure 1 shows typical pellets of glasses before and after annealing and grain growth.

## 2.2 Annealing and Grain Growth

The mixtures I and II containing titanium oxide, gallium oxide, and higher silicates were treated at high temperatures. We used a temperature range of 600°C for sintering and 750°C for the grain growth. Samples of III and IV synthesized by semiwet method were processed at 700°C.



**Fig. 1** Pellets pressed at approximately 8000 psi to prepare 12 mm diameter sample. (a) A typical size of as prepared and heat-treated glass I and II and (b) glass III and IV.

The samples were cooled by switching off the power of the furnace. Since cooling rate has pronounced effect on the morphology and glass formation, this requires further research to understand glassy and crystalline transition behavior in this material system. The pellets, shown in Fig. 1(b), were annealed to 200°C to 220°C periodically, usually for a period of 48 h. This was performed to ensure that there is no effect of moisture.

### 2.3 Thermogravimetric Analysis

The stability of samples was determined by thermogravimetric analysis using a Perkin Elmer brand Pyris 1 TGA thermogravimetric analyzer instrument. The data were collected for a heating rate of 50°C/min up to a temperature of 900°C. The change in the mass of the sample was recorded as the function of temperature.

### 2.4 Microstructural Studies

Since crystalline powder was used, a detailed the morphology of the material was studied at low magnifications (50-200X) using an optical microscope followed by scanning electron microscopy using an FEI Nova NanoSEM 450 system to image the transitioning of particles into glassy morphology. We used a 5 to 10 KeV accelerating voltage for the microstructure images. For compositional studies, we used 20 kV accelerating voltage for energy dispersive X-ray spectroscopy (Oxford Instruments X-Max 50 EDS detector). We have extensively studied the morphological transition and evolution in mixtures I and II. The detailed results of morphological transition from crystalline to glass will be reported in a future communication.

### 2.5 Electrical Characterization

The details of the dielectric constant and electrical resistivity were measured and collected using a Hewlett Packard 4263A LCR meter. The values of the dielectric constant were determined from the measured capacitance  $C$  data using the equation:

$$C = \epsilon \epsilon_0 A / d,$$

where  $\epsilon$  is the dielectric constant of the material,  $\epsilon_0 = 8.854 \times 10^{-12}$ ,  $A$  is the surface area of the prepared pellet, and  $d$  is the thickness of the pellet. We collected both dielectric constant and resistivity at several frequency ranging from 100 to 100,000 kHz and the bias voltage of 50 to 1000 mV. Resistivity was inferred from the measured resistance values at different frequency ranges.

### 2.6 Effect of High-Energy Radiation on the Glass Material

We studied the effect of high-energy radiation on bioactive glasses I and II using a commercially supplied Cs-137  $\gamma$ -radiation source which was listed for 5  $\mu$ Ci, 30.2-year half-life. The effect of radiation was evaluated before and after irradiation by measuring capacitance and resistance of the bioactive glass in the range of 50 to 1000 mV and frequencies range of 100 to 100000 Hz.



## 2.7 Spectroscopic Characterization of Bioactive Glasses III and IV

Since the behavior of bioactive glasses I and II were almost identical, we used these samples for electrical characterization. However, we listed the spectroscopic characterization of bio glasses as III and IV. The infrared spectra were determined using the Mattson Genesis II FTIR instrument. The IR spectra were then recorded from 400 to 4000  $\text{cm}^{-1}$  with a resolution of 1  $\text{cm}^{-1}$  for both irradiated and nonirradiated compositions.

## 3 Results and Discussion

All as-synthesized mixtures were compacted and annealed at 200°C followed by placing them in a furnace for sintering, complete mixing, growth, and filling the voids between neighboring particles at 750°C for the extended period. Mixtures I and II underwent a process of annealing and grain growth for a typical period of 70 to 75 h. After quenching these mixtures, the SEM morphologies had indicated the transition of the crystalline phase to the glassy phase. To ensure that mixture was completely reacted, and stable glassy behavior was achieved, we performed processing runs for up to 120 h. However, the electrical measurements showed no difference between samples processed for 70 and 120 h indicating that the stable phase was achieved in 70 h.

Figure 2 shows the microstructures of materials at various stages before formation of glassy phase. However, we observed that both glasses I and II form the faceted crystalline phases in the early stage. The hexagon formation [Fig. 2(a)] was observed for the sample at the initial stage after few hours of grain growth for the sample without selenium. As shown in Figs. 2(a) and 2(b), we observed that faceted particles are formed and do not merge easily with other grains. However, there is a greater tendency to form larger bundles of these grains in smaller sizes (300 to 700 nm size), which evolve to glassy phases. In most cases, these small grains have complex structures, mostly hexagonal morphologies. The formation of shaped and faceted grains is favored due to strong anisotropy and interface energy. Larger grains in the form of faceted particles were observed after 25 to 30 h grain growth. Coarsening mechanism and faceted

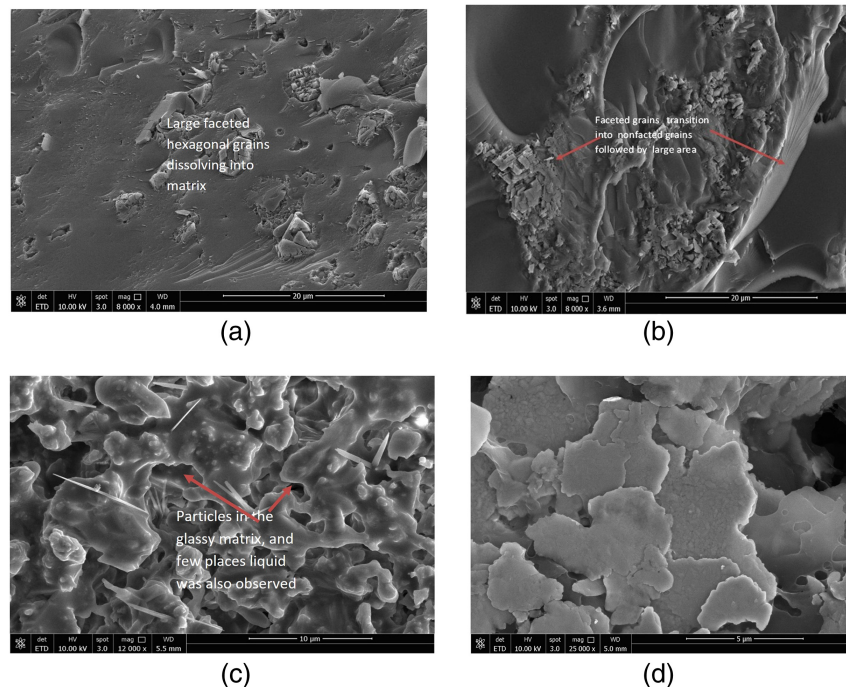


**Fig. 2** (a) Initial stage of faceted hexagonal grain formation, (b) dissolution of faceted grains and formation of glassy phase (c) microstructures of glassy phase and (d) microstructure of glass II containing titanium oxide which showed presence of particles (300 to 700 nm) trapped in glass matrix.

growth in anisotropic materials have been shown<sup>20–22</sup> during grain growth complex oxide materials. The addition of impurity<sup>20</sup> showed momentous changes in anisotropy and transition from nonfaceted to faceted grains. The details of transition of the morphology for these materials are under investigation and results will be communicated in a future communication. However, it is clear that hexagonal grains are formed in few hours of grain growth at 750°C, which ultimately dissolve and transform to nonfaceted morphology. In the composition III and IV, the glass formation in presence of selenium, growth mechanism was quite different. We observed that after sintering grains grew together and formed bunch of small grains filled with selenium liquid. Even small grains were faceted as shown in Fig. 2(b) and started merging to form glasses as the processing time was increased. Since these facets along with partial glassy phase were observed after quenching as shown in Fig. 2(c), it is clear that glass formation was favored during the fast-cooling rate as the result of quenching performed by switching off the power of the furnace. The samples treated at 750°C for 80 h followed by fast cooling did not show signs of precipitates or faceted grains. The mixture II containing titanium oxide treated for shorter time (<25 h), showed pockets of very small particles in the glass matrix [Fig. 2(c)], which disappeared in samples [Fig. 2(d)] treated for 70 h. These microstructures at large magnification did not show visible gaps. Based on the earlier observations in synthesis of calcium copper titanate materials<sup>21,22</sup> a small addition of selenium which helped in dissolving titanium oxide and formation of non-faceted grains, further study in presence of selenium may require shorter time of processing for titanium containing mixtures. In the presence of selenium, smaller grains easily were engulfed into a larger nonfaceted matrix, which changes to glassy phase.

Samples III and IV containing phosphate and borates were processed by the semiwet method before placing in furnace maintained at 700°C. The mixture was annealed for a time of 2 h followed by 70 h of grain growth. The samples III and IV contained traces of selenium, which also acted as flux and facilitates in the growth of grains, which ultimately transitioned to glasses. We observed at higher magnification materials using direct heat treatment that interfaces were smooth during the glass formation. The morphologies were determined by SEM at two different spots for samples. As shown in Fig. 3 there was no sign of precipitates or trace of faceted grains or large voids and holes in the sample. Also, the surface morphology consisted of smooth layers in the matrix of the material.

The thermal stability of the silicate materials of the compositions in Table 1 was studied by thermogravimetric analysis up to a temperature of 900°C. In the mixture III and IV phosphor-borate materials we observed material loss up to 0.32%, while for the selenium-doped material, the loss was 0.11%. There was no loss in this calcium-based silicates, indicating particularly good thermal stability. The repeated thermogravimetric studies indicated that the weight loss was very insignificant for both mixtures. Figures 4(a) and 4(b) show the typical curve for the

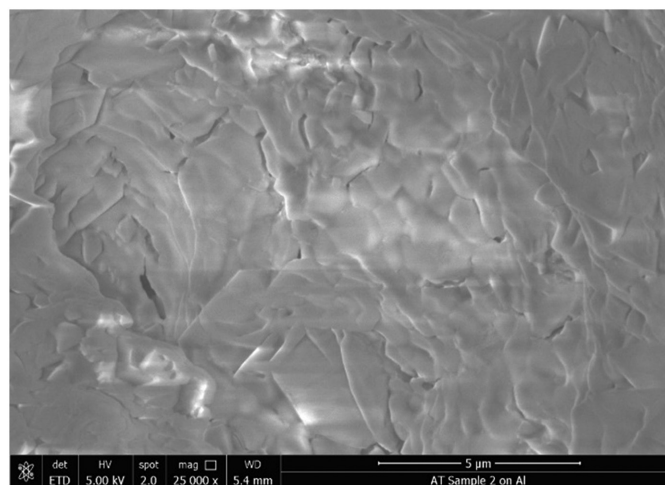


**Fig. 3** Typical morphology of glassy phase of phosphosilicates mixture synthesized by semi-wet process followed by grain growth.

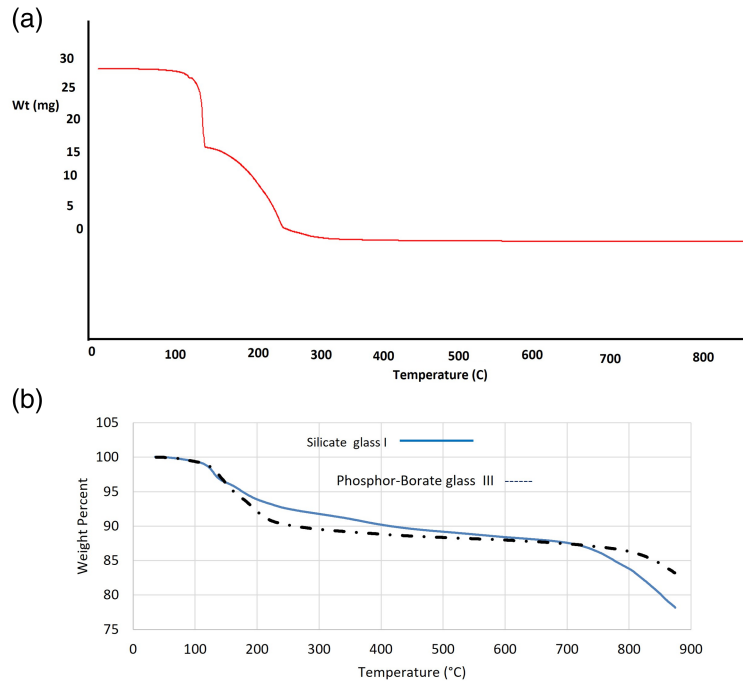


**Fig. 4** (a) Thermogravimetric data for silicate glass I and (b) phosphor-borate glasses III (blue line) and IV (green line).

silicate and phosphate glasses. The steps in Fig. 4(a) show the decomposition of small crystallites of titanium and gallium followed by a stable phase formed at elevated temperature. This is consistent with morphologies shown in Fig. 2. The thermal behavior shown in Fig. 4(b) for phosphate glass was quite different than that of high silicate containing material shown in Fig. 4(a). Figure 4(b) showed continuous decrease indicating complete glassy phase. Thermogravimetric analysis was again performed after a week and there was no difference in curves observed from the initial experiment. It shows that glasses were stable and did not change with time.

Effect of radiation on the glasses I and II were determined by measuring the capacitance and resistance of the materials before and after irradiation. The dielectric constant was determined from the capacitance data and resistivity was determined from the resistance measurements. These data were determined at room temperature. As mentioned in experimental section, we used the following equation:

$$C = \frac{\epsilon \epsilon_o A}{d},$$

for the dielectric constant where  $\epsilon$  is the dielectric constant and  $\epsilon_o \epsilon_o = 8.854 \times 10^{-12}$  F/m,  $C$  is the measured capacitance,  $A$  is the surface area of the circular facet of the pellet, and  $d$  is the thickness of the pellet. The resistivity was determined using the following equation:

$$\Omega = \frac{\rho d}{A},$$

where  $\Omega$  is the resistivity and is the  $\rho$  resistance,  $d$  is the thickness, and  $A$  is the area.

Figure 5 shows dielectric constant values for the composition I at frequencies ranging from 100 to 100,000 Hz and bias voltage of 50 to 1000 mV. We used different bias voltage to determine the breakdown of bone materials as a function of applied bias. The data showed that unlike crystalline perovskites and hydroxyapatites, the dielectric constant was approximately constant for the applied bias voltage. The applied bias voltage used in this study (50 to 1000 mV) did not affect the dielectric constant of the glasses. This suggests the stability of the glasses and indicates that there was no breakdown of the glass in this bias range. It is especially important since it shows no degradation in the glass up to the applied bias of 1000 mV. However, the glass was significantly affected by the  $\gamma$ -ray radiation even at low dose of 5  $\mu$ Ci dose. The values reported



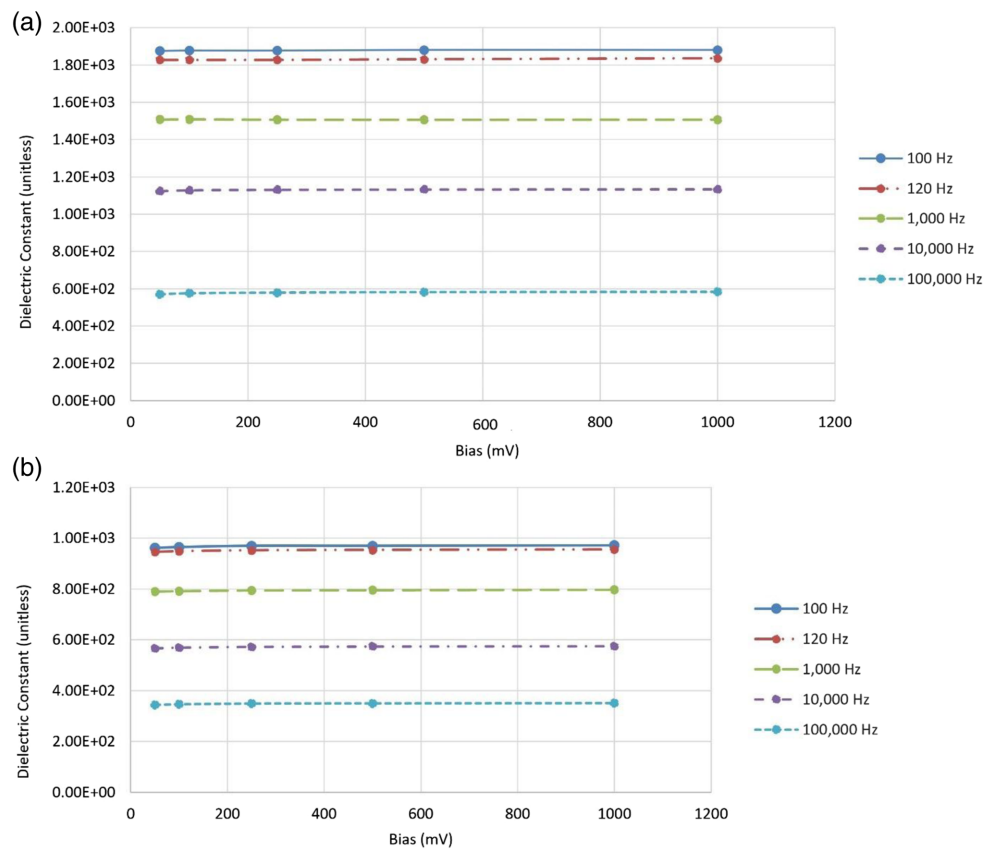


**Fig. 5** Dielectric constant of the glass sample I (a) before irradiation and (b) after irradiation at frequencies 100 to 100000 Hz and bias 50 to 1000 mV.

in Figs. 5(a) and 5(b) show the direct comparison of values for nonirradiated and irradiated samples. The dielectric values for the irradiated glass were almost half of the nonirradiated glass. This indicates that polarity of the radiated material is lower than the nonirradiated glass. These values are comparable to that of Ibrahim et al.<sup>11</sup> who had used a lithium-based system. Very similar to the dielectric values, the resistivity and hence the resistance was significantly affected by irradiation. Figures 6(a) and 6(b) show that resistivity of irradiated glass is almost three times lower for the nonirradiated bio glass. However, it is significant that these values are also constant for the applied bias voltages, indicating that glasses do not breakdown within this bias voltage range.

The effect of titanium addition had significant changes in dielectric and resistivity values. The only difference between the composition of bio glasses I and II was the addition of  $\text{TiO}_2$  in the composition of bio glass II. Previous studies<sup>20–23</sup> have shown that titanates have higher dielectric constant compared to gallates. Figure 7 shows the dielectric constant for nonirradiated and irradiated bio glasses containing  $\text{TiO}_2$ . We observed similar trends in titanate glasses also. Values were higher for the nonradiated glasses and constant as a function of the applied bias voltage. A comparison of the values is reported in Fig. 5(a) for the glass suggesting that titanate glass shown in Fig. 7(a) has significantly higher dielectric constant relative to other titanate bio glasses.

The resistivity values and hence the resistance for the bio glass II containing titanium oxide is reported in Fig. 8. A comparison of values in Figs. 8(a) and 8(b) show that the irradiated bio glass had almost three times higher resistivity relative to the nonirradiated bio glass. Similar to bio glasses I and II, the resistivity was unaffected by the bias voltage. Once again, this reaffirms that the samples do not break down within this range of applied voltages, indicating high electrical stability of these materials. The dielectric and resistance characteristics of bio glasses I and II showed similar characteristics for irradiation. Although the aim of present study was not to

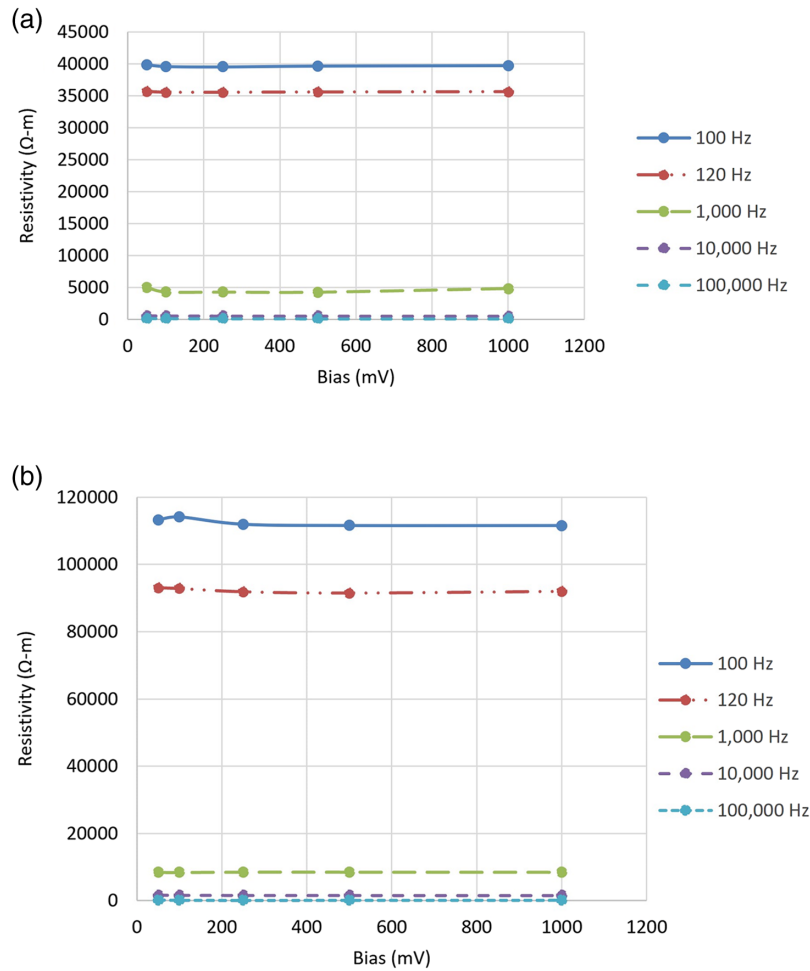


**Fig. 6** Resistivity the glass sample I (a) before irradiation and (b) after irradiation at frequencies 100 to 100000 Hz range at bias voltage of 50 to 1000 mV.

identify the contributions of grain boundaries and oxidation states on dielectric constant and resistivity, the values are attributed to the oxidation states of the glasses since there are no grains in the material.

We chose to study the optical characteristics of bio glasses III and IV. The bioactive glasses were irradiated with gamma rays and optical characteristics were evaluated in the infrared range. In this case, materials were irradiated with cobalt-60 gamma disk source, unlike the samples I and II in which we used a cesium-137 source for irradiating samples. Bio glasses III and IV were exposed to the cobalt disk, which had an area of approximately  $4.52 \times 10^{-4} \text{ m}^2$  and was calculated to have an activity of about 19.2 kBq based on its properties. The fluence for the irradiation was calculated to be approximately  $124 \text{ J/m}^2$  and the energy of radiation was about 56.0 mJ during this time. The time period for exposure was 24 h. The infrared spectra for bio glass III before and after radiation and the results are displayed in Fig. 9. Infrared spectra were determined to observe if there was breakdown of glass components which could generate new absorption peaks. We did not observe any new peak due to irradiation of the sample. The detailed studies showed that optical characteristics especially infrared spectra and Raman spectra of both III and IV bio glasses were not affected by the radiation. A few minute differences in the spectra were observed, but the discrepancies are not attributed to irradiation since the differences are not pronounced and the characteristic peaks in the spectra are preserved before and after radiation exposure. Although some of the peaks appear to be more intense in the irradiated spectrum while others appear to be less intense, the differences in relative intensity can be attributed to the angle of the incident beam and the material thickness. The polished rough surfaces and residual impurities may also have caused low intensity peaks. Extending the radiation exposure time to a

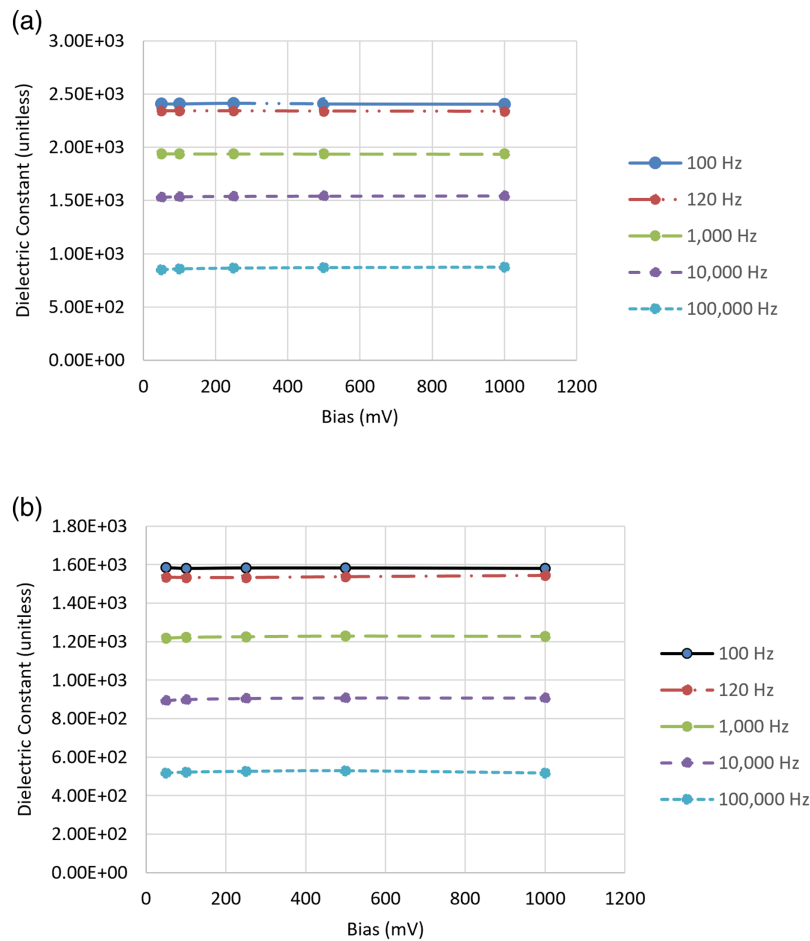


**Fig. 7** Dielectric constant of the glass sample II (a) before irradiation and (b) after irradiation at frequencies 100 to 100000 Hz and bias voltage of 50 to 1000 mV.

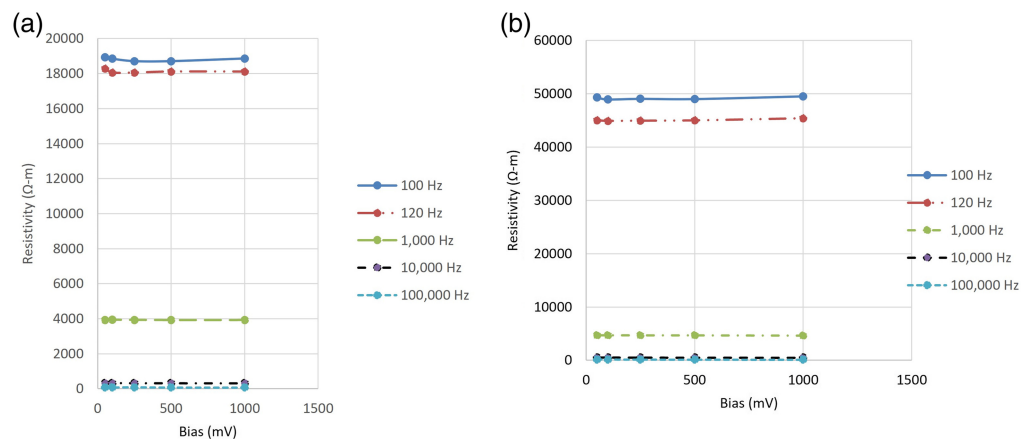


**Fig. 8** (a) Resistivity of the glass sample II (a) before irradiation and after irradiation at frequencies 100 to 100000 Hz range at bias voltage of 50 to 1000 mV.

month may have produced more profound differences in the spectra, however these studies have yet to be conducted. Raman studies were performed using a coherent brand Innova 70 argon ion laser and Acton SpectraPro 500i spectrometer cooled to  $-120.0^{\circ}\text{C}$  using liquid  $\text{N}_2$ . The laser utilized a silver mirror and a notch filter of 514.5 nm. The observed signals were very weak, very noisy, but no significant changes were observed in irradiated and nonirradiated samples of both bio glasses.

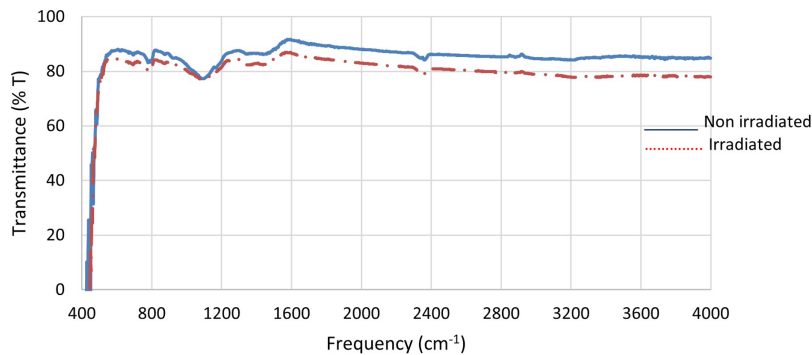


**Fig. 9** Infrared characteristics of the non-irradiated and irradiated sample; blue line shows results of non-irradiated and the (red line shows irradiated results).

## 4 Conclusions

Four hydroxyapatite silicates and phosphor borate bio active glasses were synthesized using carbonates, oxides, borate, phosphate, and silicates to study the effect of high-energy radiation. SEM morphology and EDX for each bio active glass showed that a significant time (>80 h) was required to achieve the homogeneous materials. This was needed for bio glasses in which we added gallium and titanium for their dissolution. The electrical properties including dielectric constant decreases significantly for the silicate glasses. However, the electrical resistivity increases to almost three times as high. Bioactive glasses showed very good stability since at the bias voltage of 50 to 1000 mV, both dielectric constant and resistivity were constant for a particular frequency. Similar to perovskite materials, these values decreased as we increased the frequency in the range of 100 to 100000 Hz range. The titanium containing glass had a higher dielectric constant indicating better polarity. Since in glasses there is no significant grain boundary contribution, we attribute all effects to oxidation states of the glasses. Morphology and thermal characteristic showed glass forming ability. There was some inhomogeneity in the titanium-based bio glasses which could be eliminated by longer heat treatment. The borate and phosphate glasses did not show significant difference in optical characteristics of the infrared and Raman spectra for the 24 h exposure of  $\gamma$ -ray sources. Unlike the perovskites, such as calcium copper titanates, the dielectric constant and resistivity of glassy materials did not show significant difference due to processing parameters and bias voltage.

## Code and Data Availability

All data in support of the findings of this paper are available within the article.

## Acknowledgments

Aria Tauraso thanks NASA Langley Research Center Hampton for the student fellowship. Authors are also grateful to NASA Biological and Physical Sciences Division, Headquarters for the support through the program management team of the NASA Marshall Space Flight Center Huntsville for the leverage to support students training relevant to space problems and the active technical participation.

## References

1. R. H. Hopkins et al., "Crystal growth and properties of  $\text{CaY}_4(\text{SiO}_4)_3\text{O}$  a new laser host for  $\text{Ho}^{+3}$ ," *J. Crystal Growth* **10**(3), 218–222 (1971).
2. R. H. Hopkins et al., "Silicate oxalates: new high-energy storage laser hosts for  $\text{Nd}^{+3}$ ," *J. Electro Chem. Soc.* **118**, 637 (1971).
3. K. B. Steinbruegge, "Laser properties of  $\text{Nd}^{+3}$  and  $\text{Ho}^{+3}$  doped crystals with the apatite structure," *Appl. Opt.* **11**(5), 999–1012 (1972).
4. L. L. Hench et al., "Bonding mechanisms at the interface of ceramic prosthetic materials," *J. Biomed. Mater. Res. Symp.* **5**, 117–141 (1971).
5. L. L. Hench and H. A. Paschall, "Direct chemical bond of bioactive glass-ceramic materials to bone and muscle," *J. Biomed. Mater. Res.* **7**, 25–42 (1973).

6. L. Hench, "Sol-gel materials for bioceramic applications," *Curr. Opin. Solid State Mater. Sci.* **2**(5) 604–610 (1997).
7. L. L. Hench, "Bioceramics," *J. Am. Ceram. Soc.* **81**, 1705–1728 (1998).
8. L. L. Hench and I. Thompson, "Twenty-first century challenges for biomaterials," *J. R. Soc. Interface* **7**, S379–S391 (2010).
9. V. Miguez-Pacheco et al., "Bioactive glasses in soft tissue repair," *Am. Ceram. Soc. Bull.* **94**(6), 27–37 (2015).
10. L. Hench "Bioceramics; from concept to clinic," *J. Am. Ceram. Soc.* **74**, 1487–1510 (1991).
11. S. Ibrahim et al., "Impact of high NiO content on the structural, optical, and dielectric properties of calcium lithium silicate glasses," *J. Mater. Sci.: Mater. Electron.* **33**, 10596–10610 (2022).
12. S. Singh, "Electrical properties of bone: a review," *Clin. Orthop. Relat. Res.* **186**, 249–271 (1984).
13. T. W. Balmer et al., "Characterization of the electrical conductivity of bone and its correlation to osseous structure," *Sci. Rep.* **8**, 8601 (2018).
14. B. C. Heng et al., "The bioelectrical properties of bone tissue," *Anim. Models Exp. Med.* **6**(2), 120–130 (2023).
15. B. A. M. A. Elahi et al., "A review of the dielectric properties of the bone for low frequency medical technologies," *Biom. Phys. Eng. Express* **5**(2), 02200 (2019).
16. A. S. Verma, D. Kumar, and A. K. Dubey, "Dielectric and electrical response of hydroxyapatite –  $\text{Na}_{0.5}\text{K}_{0.5}\text{NbO}_3$  bio ceramic composite," *Ceram. Int.* **45**(3), 3297–3305 (2019).
17. S. A. M. Tofail et al., "Electrical properties of hydroxyapatite," *Pure Appl. Chem.* **87**(3), 221–229 (2015).
18. H. R. Fernandes et al., "Bioactive glasses and glass-ceramics for healthcare applications in bone regeneration and tissue engineering," *Materials* **11**(12), 2530 (2018).
19. J. McAdams et al., "Effect of processing on morphology of hydroxyapatites: bioactive glasses and crystalline composites," *Proc. SPIE* **11020**, 1102006 (2019).
20. N. B. Singh et al., "Modification of interface anisotropy and its effect on microstructural evolution during Ostwald ripening," *Cryst. Res. Technol.* **48**(11), 983–988 (2013).
21. N. B. Singh et al., "Evolution of microstructure due additives and processing," *Ceram. Trans.* **235**, 65–76 (2012).
22. N. B. Singh et al., "Effect of substitution and impurities on dielectric properties and resistivity of  $\text{CaCu}_3\text{Ti}_4\text{O}_{12}$ ," *J. Emerg. Mater. Res.* **2**(6), 344–347 (2013).
23. L. Singh et al., "Progress in the growth of  $\text{CaCu}_3\text{Ti}_4\text{O}_{12}$  and related functional dielectric perovskites," *Prog. Cryst. Growth Charact. Mater.* **60**(2), 15–62 (2014).

**Aria Tauraso** is an undergraduate student at University of Maryland, Baltimore County (UMBC) majoring in physics and chemistry. During her time at UMBC, she has been active in multidisciplinary materials research. She has performed research on oxide based high dielectric materials as well as sulfide semiconducting surfaces. She has attended and presented her research results in Materials Science and Technology (MS&T 23) conference held in Columbus, OH, in 2023. She is a student member of SPIE and very active in a UMBC local chapter.

**Krishna S. Machuga** an undergraduate student at the University of Maryland College Park, Maryland, is active in multidisciplinary research and has been focusing in area of bioactive crystalline and glassy materials for bones and other bio applications. She is a coauthor in a journal paper on kidney stone materials. She has presented and published five conference proceedings and journal papers. She presented a paper and was a speaker in Materials Science and Technology (MS&T 23) in Columbus Ohio and published her research in SPIE Proceedings. She is a student member of SPIE.

**Joel McAdams** received his BS and MS degrees from the Chemistry Department of the University of Maryland Baltimore County, Baltimore, MD. After completing his MS degree at the University of Maryland Baltimore County, he joined as an analytical chemist and was promoted to associate manager for analytical services. At present, he is a senior scientist and is responsible for analytical chemistry responsibilities. His research is presented in the SPIE meetings and was published in SPIE proceedings.

**Ching Hua Su** is a materials scientist at NASA/Marshall Space Flight Center Huntsville, Alabama. He received his BS degree in materials science and engineering in 1976 and his PhD in materials science and metallurgy from Marquette University in 1985. He is author or co-author of more than 100 peer-reviewed journal articles. His current research interest includes



crystal growth in microgravity environment on International Space Station and materials processing for thermoelectric applications. He has developed, pioneered physical vapor transport methods, and demonstrated growth of chalcogenides and chalcopyrites for optical and electronic applications. Several of his papers and NASA reports have resulted in microgravity experiments to understand the role of thermal and solutal convection during crystal growth. He has been very instrumental in supporting undergraduate and graduate students focusing on the materials to meet the critical needs of NASA and country.

**Brian Cullum**, head Department of Chemistry and Biochemistry at the University of Maryland Baltimore County, received his BS degree in chemistry from Frostburg State University and PhD degree in analytical chemistry/optical spectroscopy from the University of South Carolina to develop optical sensors and optical sensing techniques for both environmental and combustion monitoring. After his PhD, he was a postdoctoral fellow in the Life Sciences Division at Oak Ridge National Laboratory. Currently he heads up the interdisciplinary Center for Translational Nano bioscience there, which is focused on development and application of nanotechnology for biomedical and defense related applications. He has served as conference chair of SPIE's Smart Biomedical and Physiological Sensor Technologies Conference for the past ten years, acted as a project consultant for NATO's Science for Peace Program, and has authored or co-authored more than 75 peer-reviewed publications, 11 book chapters and 9 edited books on these topics. He has two patents in surface enhanced Raman scattering (SERS) and SERS nano-imaging, as well as an IR-100 award and numerous other awards, including a Fellow of SPIE and a Fellow of Optica.

**Tagide deCarvalho** is the assistant director of the CNMS Core Facilities and manager of the Keith R. Porter Imaging Facility. She obtained a PhD in behavior, evolution, ecology, and systematics from the University of Maryland, College Park. Following her PhD, she was a post-doctoral fellow in the Department of Embryology at the Carnegie Institution for Science in Baltimore. She has over 10 years of experience in optical and electron microscopy for both biological and materials science research. She is considered an expert in bacteriophage imaging and currently works with at least 20 different institutions on their SEA-PHAGE courses (Science Education Alliance-Phage Hunters Advancing Genomics and Evolutionary Science), which has resulted in several publications. She also works at the intersection between art and science, and her internationally award-winning images have been featured in textbooks, a NASA calendar and USPS stamps.

**Narasimha S. Prasad** received his PhD in nonlinear optics from the Klipsch Department of Electrical and Computer Engineering, New Mexico State University, in 1994. He joined NASA Langley Research Center in 2004 as an aerospace technologist in the Laser Remote Sensing Branch of the Engineering Directorate. Previously, he was a senior research scientist at Coherent Technologies, Inc., Louisville, CO (1997–2004) and a senior research physicist at Petrolaser, Inc., Las Cruces, NM (1991–2004). He has more than 30 years of R&D experience. He has expertise in lasers, nonlinear optics, remote sensing systems and components, nanotechnology, spectroscopy, and optical instrumentation. He has been a principal investigator or technical lead on numerous NASA-sponsored projects. He has published more than 180 papers, has 11 patents, and author of more than 25 technical reports. He is a senior member of OSA and SPIE. He has won several performance awards including the NASA Innovator award (2023).

**Bradley Arnold** is a member of SPIE. He received his PhD in chemistry from the University of Utah. Before joining the Chemistry Department of the University of Maryland, Baltimore County, he was a post-doctoral fellow at the University of Rochester. His research group has extensive expertise in the application of ultra-fast laser techniques to explore photochemical reaction mechanisms. He has developed applications of time-resolved linear dichroism spectroscopy to gain an understanding of the orientational aspects of electron and energy transfer reactions. These studies have focused on the orientation of photoproducts relative to the initial orientation of the starting materials to obtain important mechanistic information. More recently he has established a research program aimed at developing coherent back-scattered laser spectroscopy as a potential method to detect analytes in the vapor phase. Temporal and spatial focusing of high power ultra-short laser pulses are used to measure stimulated Raman scattering, laser induced plasma emissions, multi-photon absorption, and laser induced fluorescence. He has published

more than 50 journal articles and has been supervising students in the field of optics and photonics. He is highly active member of the American Chemical Society and has chaired the eastern section of the society.

**Fowl-Sen Choa** received his BS degree from National Taiwan University and his MS and PhD degrees from SUNY at Buffalo. After his PhD research work on femtosecond infrared lasers and detectors, in 1988 he joined AT&T Bell Labs at Holmdel and Murray Hill, NJ, and worked in photonic integrated circuits and chemical beam epitaxy. Since joining UMBC in 1991, he has been working in the areas of III-V compound semiconductor material growth and processing, broadband WDM switches and networks, RF-photonics components and systems, quantum cascade lasers, photon counting avalanche photodiodes and arrays, photoacoustic sensing, imaging, and acoustic array transmissions and receiving. Since 1991, he has been sponsored and co-sponsored with a total of more than \$14 million in research funding from diverse sources, including an MOCVD crystal growth facility built at UMBC. He has authored and co-authored more than 300 refereed publications. He is a fellow of OSA, a fellow of SPIE, a senior member of IEEE, an associate editor of the *Journal of High-Speed Networks*, and has been a topical editor of *Optics Letters* for 6 years.

**Kamdeo Mandal** is a senior professor in the Department of Chemistry of the Indian Institute of Technology, Banaras Hindu University, Varanasi. He received his BSc and MSc degrees from Bhagalpur University and his PhD in the Chemistry Department of the Banaras Hindu University. He is a fellow of the Royal Society of Chemistry. He has published more than 300 journal and conference papers, presented more than 85 invited and plenary lectures and has been awarded for his innovative semiwet technique for development of perovskites for electrical energy storage. He has supervised more than 20 PhD students, given more than 30 invited and plenary lectures. Published more than 200 journal and conference papers, he is in the organizing committee of international conferences, and he was the chairman of the international conference and arranged an international conference in Indian Institute of Technology BHU Varanasi attended by national and international participants.

**Narsingh B. Singh** a research professor in the Department of Chemistry and Biochemistry, and Department of Computer Science and Electrical Engineering of the UMBC, received his BSc, MSc and PhD degrees in chemistry from Gorakhpur University, India. He is a fellow of SPIE, fellow of the American Society of Materials (ASM) International, fellow of the Optical Society of America, and fellow of the Royal Society of Chemistry (RSC), is internationally recognized for the managerial leadership and research in materials science and engineering. He held the position of the “Senior Consulting Engineer” the highest technical position in the Northrop Grumman Electronic Systems at Baltimore Maryland until December 30, 2011. He has published more than 300 journal and conference papers, presented more than 85 invited and plenary talks, has 25 issued patents and more than 250 company trade secrets and invention awards. He has been associate editor of the *Progress in Crystal Growth and Characterization* for more than three decades and he is in the editorial board of several other journals. He served the National Academy of Sciences as a panel member on the National Materials Advisory Board for many years. He is the founder of the Northrop Grumman Materials Corporate Forum, which focuses on critical materials technologies for the corporation and holds yearly conference for Northrop Grumman researchers.